Title
Ellipsometry of human tears.

Journal
The ocular surface, 17(2)

ISSN
1542-0124

Author
Glasgow, Ben J

Publication Date
2019-04-01

DOI
10.1016/j.jtos.2019.02.008

Peer reviewed

HHS Public Access

Author manuscript

Ocul Surf. Author manuscript; available in PMC 2020 April 01.

Published in final edited form as:

Ocul Surf. 2019 April ; 17(2): 341–346. doi:10.1016/j.jtos.2019.02.008.

Ellipsometry of Human Tears

Ben J. Glasgow[1]

[1]Departments of Ophthalmology, Pathology and Laboratory Medicine, Jules Stein Eye Institute, 100 Stein Plaza, University of California, Los Angeles CA 90095, USA

Abstract

Purpose—The outer surface layer tears is presumably composed of lipid. The thickness of this layer is considered critical to retard evaporation. Prior thickness measurements differ widely. Advances in ellipsometry have availed more precise and accurate measurements for thin films. The range in thickness of the surface layer of tears was studied by ellipsometry to uncover the source of prior discrepancies.

Methods—Tear surface layers of normal and dry eye subjects were measured by in-vitro ellipsometry. Lateral and Z resolutions of ~ 1 micron and 0.1 nm, were achieved respectively. Thicknesses were derived from matrices and a Levenberg–Marquardt multivariate regression algorithm to Fresnel equations for multi-layered films.

Results—Ellipsometric measurements of pooled and individual human tears in-vitro revealed a larger overall range (2.6-500 nm) of surface film thicknesses than previously reported by any one study. Each sample showed thin areas (0-2.6 nm) with interspersed thicker regions (~200-500 nm). Repeat measurements of a single donor collected at weekly intervals showed a broad range of surface thicknesses within and between samples. Thickness measurements from a dry eye subject overlapped that of normal subjects.

Conclusion—The data show that published disparity in surface film thickness may be attributable to limitations of prior methodologies. The range and overlap of surface film thicknesses challenge less rigorous methodologies that claim to segregate normal and dry eye.

Keywords

dry eye; ellipsometry; interferometry; lipid layer thickness; Meibomian lipid; reflectometry; tear thickness

Corresponding author- Ben J. Glasgow, bglasgow@mednet.ucla.edu, FAX-none, Telephone (310) 825-6261.

5. Disclosures/Conflicts of Interest

The author reports no conflicts of interest.

1. Introduction

The tear film has been classically modeled as 3 distinct layers. Historically, the surface layer is presumed to be composed of lipid. This conclusion is based on the observation of interference fringes on the aqueous layer [1]. The lipid layer is considered to be critical for retardation of evaporation. The thickness of the surface layer of tears has been suggested as a criterion to distinguish dry eye disease from normal subjects and to evaluate therapy for dry eye disease [2–4]. Understanding the normal range of surface film thickness is crucial to these applications. However, a review of the representative studies show substantial variation in the reported thickness of the surface tear film layer (Table 1).

The reported variation must be considered in light of the techniques used for these measurements. Most methodologies are inherently restricted to specific ranges of wavelength that result in color. For example, methods based on color interferometry are limited by the color spectrum and the range is limited to integers of ½ wavelength. Observed color in a thin film occurs cyclically at thicknesses that vary by hundreds of nanometers [14]. Within a single color range the thickness may vary by increments of 20-100 nanometers. Colors are not usually observed below a threshold on the order of 150-200 nm [15]. Therefore, judging the thickness of a surface film by its color is fraught with potential error.

Further complications may arise in the methods used for fitting. Most algorithms in interferometry and reflectometry require an initial estimation of thickness. Mis-estimation risks finding local minima closest to the assumed thickness. Ellipsometry has a significant advantage over these techniques. Ellipsometry measures the degree of phase shift as light is reflected from a surface film, which markedly increases sensitivity over a reflection measurement. Further, unlike most reflectometers, ellipsometers measure more than a single amplitude parameter. For each point of measurement ellipsometry fits both phase and polarization amplitudes to generated local fits for multiple wavelengths and/or incident angles [16]. This data set permits a global fit for a true minimum. Another source of error in clinical studies is error related to the measurement environment. Most tear film surface thickness measurements have been performed in-vivo. Clinical measurements are subject to dynamic changes from tear film thinning, motion of the eye, and eyelids, as well as tear film angular deviations from menisci and corneal curvature. The lateral resolution in such dynamic environments is diminished. The inescapable result is that clinical measurements reflect an average over a relatively large region of interest. Many of these problems are minimized when measurements are performed in-vitro.

Recent advances in measurement of thin films have been driven by the semi-conductor industry. The result is improved instrumentation and software for metrology. These innovations have led to high lateral (on the order of a micron) and excellent z resolutions (sub-nanometer) [17]. Computationally challenging fitting has been facilitated for complex models and can even be mapped for thickness measurements at each pixel. Global fitting algorithms have been thoroughly vetted. Thicknesses can be accurately measured over a range of less than 1 nm to many microns. This range exceeds that provided by currently available techniques in use for tear films. These advances in ellipsometry were applied to

measurements of the human tear film to investigate the sources of variation in thickness in prior studies.

2. Methods

2.1 Tear collection

Stimulated human tears were collected from healthy volunteers in accordance with the tenets of the Declaration of Helsinki and approved by the institutional review board. Informed consent was obtained from donors after explanation of the nature and possible consequences. Human subjects were screened for symptoms of dry eye disease as previously described [18]. One subject met the criteria for mild to moderate dry eye on the basis of symptoms, punctate corneal fluorescein staining, a tear breakup time of 5 seconds, and a Schirmer's test of 0-2 mm (repeated on 3 separate occasions). Slit lamp examination of the tarsal conjunctiva revealed disrupted Meibomian gland in focal areas. Stimulated tears were collected as previously published with polished glass tips and glass transfer pipettes [19]. Tears from 30 normal subjects (ages 19-25) were pooled into three lots of ten subjects each in polytetrafluoroethylene-lined glass vials and stored under nitrogen at −80C until use. Tears from single donors were pipetted directly into the sample chamber for immediate ellipsometry measurement.

2.2 Sample chamber

The sample holder was fabricated from a 25 mm diameter × 10 mm length disc of black polyether ether ketone thermoplastic polymer to vitiate the menisci at the water-lipid interface. The tear samples were placed in an internally milled cylindrical sample chamber of 12.5 mm diameter × about 2 mm in depth. The bottom of the sample chamber was skewed at an angle to minimize reflection from that surface. The minimum volume of tears necessary for an adequate signal in the chamber was about 200 uL.

2.3 Ellipsometry

Imaging ellipsometry measurements were obtained with an imaging nulling ellipsometer nanofilm-EP4 (Accurion Gmbh, Gottingen, Germany) at 20°C. Polarizer and analyzer angles were determined under the nulling conditions for each region of interest (ROI) with a Nikon 20× objective. Measurements were made in two modes to obtain both overall average and detailed point to point mapping in ROIs.

Variations between ROIs of the same sample were observed by constructing thickness maps scanning an area of up to 300 × 300 microns. Thickness measurements and maps were made in the nulling mode with a 658 nm 50mW laser light source. Angular measurements of the polarizer and analyzer reflect the polarization and phase shift, and are referred to as psi (Ψ) and delta(Δ). Ψ and Δ values were measured at each pixel in different ROIs of the scan. The lateral resolution approximates 1 μm as given by the overall resolution provided by the optics in the reflected light beam. Measurements were collected at 1 degree intervals of incident angles between 50-57 degrees. The data were modeled for a lipid surface layer under air and over an aqueous substrate (index of refraction, n=1.333), all considered transparent films in the model. The refractive index was also separately tested for fit using

the stacked layered model [16]. The optical constant n=1.491 for the 658 nm wavelength matched that given for Meibomian lipids [20]. The reflectance (r) matrix is described by the ratio $\rho = r_p/r_s = \tan \Psi\ e^{i\Delta}$ where the amplitude of the parallel (*p*) and orthogonal (*s*) components of the reflected light are normalized to initial amplitude of the incoming light with the ellipsometric angles Ψ and Δ, respectively. To derive thickness measured ellipsometric angles Ψ and Δ were parameters input into the Accurion proprietary modeling software (EP4Model software), that uses a Berreman matrix algorithm for multilayered films fitting and a Levenberg–Marquardt multivariate regression algorithm to Fresnel equations for multilayered films [16,21]. The material stack included successive layers of air lipid and water. Negative control substrates included water and tear mimicking buffer, devoid of a surface layer. Positive controls consisted of oleic acid and 1,2 dipalmitoyl-sn-glycero-3-phosphatidyl choline (DPPC), (Avanti Polar lipids, Inc, Alabaster, AL) monolayers on the negative controls substrates. Lipids dissolved in 1ul of hexane and chloroform were layered on the substrates. The lipids were gravitometrically measured to just cover the surface area of the sample chamber as described [22,23]. In keeping with the purpose of discerning the variation within and between samples, calculated thickness are reported herein generally as a range rather than average thicknesses with root mean square error values. A minimum of 6 measurement scans were made from each sample in regions that encompassed the thinnest and thickest measurements. A minimum of 4 areas were scanned in each sample. The system was initially calibrated with a silicone dioxide wafer of known surface layer thickness.

3. Outcome data

3.1 Resolution of monolayer surface films by ellipsometry

The control substances were chosen to validate the resolution of the ellipsometer for surface films in solution. For monolayers oleic acid and a phospholipid were chosen. Oleic acid is the principal component of the first substances for which monolayers were recognized and characterized [23][22]. The thickness obtained for this monolayer (Table 2) matches that previously published. Similarly, the monolayer of DPPC matches the expected value (Table 2) and demonstrates the z resolution available by ellipsometry [24]■ .

3.2 Precision of tear surface film thickness

The data for range of thicknesses found in the controls and various tear samples are summarized in Table 2. To determine the precision of individual measurements, scans were repeated over one field of one subject’s tears 7 times within about 10 minutes. The range for the average measurements from these scans was 17.6-20.5 nm, mean ± standard deviation = 19.4 ± 1.1 nm. The measurements in the same ROI showed a similar range of about 0-105 nm with high end of the range varying only between 90-110 nm. Despite unavoidable diffusion of the molecules in the surface layer the measurements are highly precise.

The values obtained for individual tear samples vary widely and cover the overall published range when considered as a group (Table 1). The low end value of 2.6 nm this matches published estimates done by Brewster angle microscopy and vibrational analysis [10,11]. Although this early published work has been largely overlooked in the current literature, the

data depict the thinnest areas of the surface layer of the tear film. In more recent work, King-Smith et al. acknowledged that regions of the tear film surface layer may be thinner than 20 nm or greater than 120 nm, but was unable to achieve measurements beyond these limits of resolution with a home built reflectometer. The ellipsometer is very accurate at the low end of measurement. Ellipsometry has been predicted to have an uncertainty of ± 0.025 and ± 7 nm for lipid refractive index and lipid thickness, respectively for clinical measurements of a tear film thickness of 150 nm [25]. The measurement of 2.6 nm in tears achieved by ellipsometry is consistent with a monolayer or bilayer depending orientation and chain length of the molecules that compose those regions. Only one very early study roughly predicted the upper limit of the range (~500 nm) for the tear film observed in the current study (Table 1). The probable explanation for bias toward the lower range in many studies involves the cyclical nature of the color interference phenomenon as described in Newton's fringes. The assumption of the lowest fractional integer for any specified color for fitting purposes will of course exclude the same color with a higher fractional integer of a thicker layer [14]. A global fit vitiates this problem.

The heterogeneity of individual samples is best visualized by maps of the surface layer of the tear film. The high contrast image from ellipsometry of an exemplary lot of pooled tears is shown in Figure 1. The predominance of the dark areas indicate very thin layers with much thicker islands of lipids. These areas both were fit to a refractive index of 1.491, consistent with the reported refractive index for meibomian lipids [20].

3.3 Comparison of surface film thickness by ellipsometry to prior studies

Most studies report averages rather than ranges or distribution maps of thickness. However, the range may be more important to assess overlap. There is one notable exception [13]. The excellent maps gathered by King-Smith et al. include description of islands of thick lipids rising from a sea of lower thickness. These observations match the ellipsometric pattern of raised aggregates in a background of a thinner film. Although the z resolution in the study by King-Smith et al. was limited to greater than 20 nm and less than 120 nm, the authors astutely describe the variation in clinical measurements. The concordance of their in-vivo thickness measurement with those of the in-vitro sample here was reassuring.

Aggregation of tear lipids on surface films has also been seen in model systems. Meibum is known to form heterogeneous surface films including regions with monolayers and aggregates of multilayers of molecules in Brewster angle microscopy [24–29]. Squalene forms lenses and aggregates with compression in Langmuir trough studies [30]. In vitro studies have demonstrated that meibum spread as thin films yield surface films of 5.2 nm in thickness [33]. Metrology performed here on tears reaffirm the heterogeneous nature of the surface film created by meibum and provide a broader range of thicknesses. A methodologic concern for the collection of pooled stimulated tears is that a narrow and deep storage container might not reflect the amount of lipid that exists clinically. However, the in-vitro methods appear to be reassuringly consistent to the findings in-vivo.

3.4 Ellipsometry of the surface layer of freshly collected tears in individuals

To gain further insight individual tear samples were collected without pooling or storage and immediately studied by ellipsometry. Even though stimulated tears are dilute the amount of lipid present obtained during collection at least should reflect the amount on the surface of tears initially. The rationalization was that lipid would rise to the surface and provide a similar amount to that present clinically. Further, the surface area of the sample container was designed to approximate that of the cornea. The individual samples showed a range of thickness greater than that of the pooled tears (Table 2). One explanation for a greater thickness in the unstored samples is that some surface film molecules may be lost in the process of freezing and storing the pooled lots. Alternatively, the greater range may simply represent natural variation in the samples. As a test, fresh tears from the same individual were collected and measured in 3 successive weeks. The surface film thickness of tears from this individual varies greatly from week to week (Figures 2 and 3). The surface film thickness measured one week was less and another week greater than that observed with the pooled frozen stored lots. The low end of the range < 5 nm was seen in each case in the maps of freshly collected samples. Again the patterns observed from ellipsometric imaging resemble both the form and variation as previously described [13]■ .

3.5 Ellipsometry of the surface film of tears from a patient with dry eye

Only one subject who met the criteria for mild to moderate dry eye provided enough tears for immediate study by ellipsometry. The range overlapped that of thickness of normal individual subjects here and that reported in prior studies (Tables 1 and 2). Figure 4 shows the thickness map. Within the ROI a large range of thickness was observed. The average thickness (mean of about 36 nm) of the dry eye subject was higher than that of 2 of the 4 normal subjects. One possible explanation for overlap with normal subjects is the dry eye disease of this subject may be aqueous deficiency rather than meibomian gland disease. However, the measured average tear surface film thickness of the dry eye patient and 2 of the normal subjects would have been under the 75 nm or even 60 nm cut-off values for the detection of meibomian gland disease[34].

3.6. Unusual finding of focal baseline shifts

One subtle finding was observed in focal regions of the thickness maps. The baseline appears shifted upward (Figures 2a, 3a, 4a). The shifts are generally focal and minimal (1-2 nm) and correction did not significantly affect the calculated average or the range. However, in these areas the subphase n=1.33 is not uniform and the superficial layer n=1.49 appears pushed upward. To highlight this finding these areas were not normalized to baseline. Possible explanations include contamination with debris localized to the interface of the surface and subphase or perhaps molecules penetrating the surface such as proteins. The ladder explanation has been suggested as proteins unfolding at the surface in Langmuir trough in-vitro studies [35,36], but has not been shown before in tears samples. The exact biochemical nature of the molecules responsible for the shift will require further investigation. The finding has not been previously reported with other instruments for surface film measurements of tears.

3.7 Implications

The importance of determining the range of normal thickness is important because instruments used for surface film thickness measurements often assume there is a lower limit to normal thickness, e.g., less than 100nm or 75 is abnormal [3,34]. The presence of surface film molecular aggregates and the intra- and inter-subject variation both in-vitro and in-vivo with high resolution ellipsometry challenge prior comparisons for normal and dry eye measurements [4]. The data presented here expand the range of variability within samples described by King-Smith et al. [13]. The overlap in the measured thicknesses in-vivo may be dependent on temporal and spatial considerations. The data in-vitro without motion show even larger variation and overlap between individuals. The variability of tear surface film thickness, as currently measured, is unlikely to be useful to segregate dry eye disease.

3.8 Shortcomings of in-vitro and in-vivo measurements

Both in-vivo and in-vitro measurements have method-related shortcomings. The motion of the subject, eye, tear film in clinical measurements on a curved surface reduce precision and accuracy. In vitro measurements are made on relatively static films in controlled environments. In vitro measurements are less vulnerable to dynamic variation but may not recapitulate the clinical situation and require more sample. In this study, some reassurance is gained for implementing in vitro studies as a model. The general range of thicknesses match that of published clinical studies when the data are viewed as a whole. One might argue that stimulated tears dilute lipids resulting in lower thicknesses than observed clinically. Conversely, one could claim that multiple collections concentrate lipids to excess on the surface film. But the ellipsometric data show an extended the range of thickness of each sample at both higher and lower limits compared to clinical studies. Differences cannot be attributed to a consistent bias from the in-vitro collection, preparation or measurement.

4. Summary and Conclusions

The findings here do not necessarily render tear surface film thickness measurements unimportant. The relevance of thickness measurements must be considered in the context of overall lipid production. Individual thickness measurements are made in very short time frame and may not reflect overall lipid excretion. The time scale of point measurements for both in-vivo and in-vitro methods are roughly on the order of seconds or less. Perhaps surface layer thickness differences should be considered on a much longer time scale of hours to days. In this case, an approach to integrate clinical thickness measurements over a much longer duration might possibly reveal differences between normal and dry eye patients.

Acknowledgments

This work was supported by the National Institutes of Health, EY 11224 and the Edith and Lew Wasserman Professorship.

Funding: This work was supported by the National Eye Institute, Grant-EY11224 and the Edith and Lew Wasserman Professorship.

6. References

[1]. McDonald JE. Surface phenomena of the tear film. Am J Ophthalmol 1969;67:56–64. [PubMed: 4178152]

[2]. Olson MC, Korb DR, Greiner JV Increase in tear film lipid layer thickness following treatment with warm compresses in patients with meibomian gland dysfunction. Eye Contact Lens 2003;29:96–9. doi:10.1097/01.ICL.0000060998.20142.8D. [PubMed: 12695712]

[3]. Ji YW, Lee J, Lee H, Seo KY, Kim EK, Kim T. Automated Measurement of Tear Film Dynamics and Lipid Layer Thickness for Assessment of Non-Sjögren Dry Eye Syndrome With Meibomian Gland Dysfunction. Cornea 2017;36:176–82. doi:10.1097/ICO.0000000000001101. [PubMed: 28060064]

[4]. Blackie CA, Solomon JD, Scaffidi RC, Greiner JV, Lemp MA, Korb DR. The relationship between dry eye symptoms and lipid layer thickness. Cornea 2009;28:789–94. doi:10.1097/ICO.0b013e318191b870. [PubMed: 19574906]

[5]. Tung CI, Kottaiyan R, Koh S, Wang Q, Yoon G, Zavislan JM, et al. Noninvasive, objective, multimodal tear dynamics evaluation of 5 over-the-counter tear drops in a randomized controlled trial. Cornea 2012;31:108–14. doi:10.1097/ICO.0b013e31821ea667. [PubMed: 22138585]

[6]. Huang J, Hindman HB, Rolland JP. In vivo thickness dynamics measurement of tear film lipid and aqueous layers with optical coherence tomography and maximum-likelihood estimation. Opt Lett 2016;41:1981. doi:10.1364/OL.41.001981. [PubMed: 27128054]

[7]. Hwang H, Jeon H-J, Yow KC, Hwang HS, Chung E. Image-based quantitative analysis of tear film lipid layer thickness for meibomian gland evaluation. Biomed Eng Online 2017;16:135. doi:10.1186/s12938-017-0426-8. [PubMed: 29169367]

[8]. Norn MS. Semiquantitative interference study of fatty layer of precorneal film. Acta Ophthalmol 1979;57:766–74. [PubMed: 525300]

[9]. Korb DR, Baron DF, Herman JP, Finnemore VM, Exford JM, Hermosa JL, et al. Tear film lipid layer thickness as a function of blinking. Cornea 1994;13:354–9. [PubMed: 7924337]

[10]. Kaercher T, Möbius D, Welt R. Biophysical characteristics of the Meibomian lipid layer under in vitro conditions. Int Ophthalmol 1992;16:167–76. [PubMed: 1452421]

[11]. Kaercher T, Hönig D, Möbius D, Welt R. [Morphology of the Meibomian lipid film. Results of Brewster angle microscopy]. Ophthalmologe 1995;92:12–6. [PubMed: 7719067]

[12]. Goto E, Tseng SCG Differentiation of lipid tear deficiency dry eye by kinetic analysis of tear interference images. Arch Ophthalmol (Chicago, Ill 1960) 2003;121: 173–80.

[13]. King-Smith PE, Nichols JJ, Braun RJ, Nichols KK. High resolution microscopy of the lipid layer of the tear film. Ocul Surf 2011;9:197–211. [PubMed: 22023815]

[14]. Kitagawa K Thin-film thickness profile measurement by three-wavelength interference color analysis. Appl Opt 2013;52:1998. doi:10.1364/AO.52.001998. [PubMed: 23545954]

[15]. McDonald JE. Surface phenomena of tear films. Trans Am Ophthalmol Soc 1968;66:905–39. [PubMed: 4181023]

[16]. Tompkins HG, Irene EA. Handbook of Ellipsometry. vol. 30 William Andrew, Inc. and Springer-Verlag GmbH & Co KG; 2005. doi:10.1016/0895-7177(95)00047-6.

[17]. Losurdo M, Bergmair M, Bruno G, Cattelan D, Cobet C, de Martino A, et al. Spectroscopic ellipsometry and polarimetry for materials and systems analysis at the nanometer scale: state-of-the-art, potential, and perspectives. J Nanoparticle Res 2009;11:1521–54. doi:10.1007/s11051-009-9662-6.

[18]. Mokhtarzadeh M, Casey R, Glasgow BJ. Fluorescein punctate staining traced to superficial corneal epithelial cells by impression cytology and confocal microscopy. Investig Ophthalmol Vis Sci 2011;52:2127–35. [PubMed: 21212176]

[19]. Dean AW, Glasgow BJ. Mass spectrometric identification of phospholipids in human tears and tear lipocalin. Investig Ophthalmol Vis Sci 2012;53:1773–82. doi:10.1167/iovs.11-9419. [PubMed: 22395887]

[20]. Tiffany JM. Refractive index of meibomian and other lipids. Curr Eye Res 1986;5:887–9. [PubMed: 3780283]

[21]. Goldhahn R Dielectric Function of Nitride Semiconductors: Recent Experimental Results. Acta Phys Pol A 2003;104:123–47. doi:10.12693/APhysPolA.104.123.

[22]. Wang D-N, Stieglitz H, Marden J, Tamm LK. Benjamin Franklin, Philadelphia's favorite son, was a membrane biophysicist. Biophys J 2013;104:287–91. doi:10.1016/j.bpj.2012.12.028. [PubMed: 23442850]

[23]. Pockels A Ten Years of Research in One Paper. Nature 1891 ;46:437–9.

[24]. Kienle DF, de Souza JV, Watkins EB, Kuhl TL. Thickness and refractive index of DPPC and DPPE monolayers by multiple-beam interferometry. Anal Bioanal Chem 2014;406:4725–33. doi: 10.1007/s00216-014-7866-9. [PubMed: 24842403]

[25]. Kottaiyan R, Yoon G, Wang Q, Yadav R, Zavislan JM, Aquavella JV Integrated multimodal metrology for objective and noninvasive tear evaluation. Ocul Surf 2012;10:43–50. doi:10.1016/j.jtos.2011.12.001. [PubMed: 22330058]

[26]. Georgiev GA, Yokoi N, Ivanova S, Tonchev V, Nencheva Y, Krastev R. Surface relaxations as a tool to distinguish the dynamic interfacial properties of films formed by normal and diseased meibomian lipids. Soft Matter 2014;10:5579–88. doi:10.1039/C4SM00758A. [PubMed: 24959988]

[27]. Ivanova S, Tonchev V, Yokoi N, Yappert MC, Borchman D, Georgiev GA. Surface Properties of Squalene/Meibum Films and NMR Confirmation of Squalene in Tears. Int J Mol Sci 2015;16:21813–31. doi:10.3390/ijms160921813. [PubMed: 26370992]

[28]. Georgiev GA, Eftimov P, Yokoi N. Structure-function relationship of tear film lipid layer: A contemporary perspective. Exp Eye Res 2017;163:17–28. doi:10.1016/j.exer.2017.03.013. [PubMed: 28950936]

[29]. Nencheva Y, Ramasubramanian A, Eftimov P, Yokoi N, Borchman D, Georgiev GA. Effects of Lipid Saturation on the Surface Properties of Human Meibum Films. Int J Mol Sci 2018;19:2209. doi:10.3390/ijms19082209.

[30]. Svitova TF, Lin MC. Dynamic interfacial properties of human tear-lipid films and their interactions with model-tear proteins in vitro. Adv Colloid Interface Sci 2016;233:4–24. doi: 10.1016/j.cis.2015.12.009. [PubMed: 26830077]

[31]. Mudgil P, Millar TJ. Surfactant properties of human meibomian lipids. Invest Ophthalmol Vis Sci 2011;52:1661–70. doi:10.1167/iovs.10-5445. [PubMed: 21051693]

[32]. Ivanova S, Tonchev V, Yokoi N, Yappert MC, Borchman D, Georgiev GA. Surface Properties of Squalene/Meibum Films and NMR Confirmation of Squalene in Tears. Int J Mol Sci 2015;16:21813–31. doi:10.3390/ijms160921813. [PubMed: 26370992]

[33]. Millar TJ, King-Smith PE. Analysis of Comparison of Human Meibomian Lipid Films and Mixtures with Cholesteryl Esters In Vitro Films using High Resolution Color Microscopy. Investig Opthalmology Vis Sci 2012;53:4710. doi:10.1167/iovs.12-10022.

[34]. Finis D, Pischel N, Schrader S, Geerling G. Evaluation of Lipid Layer Thickness Measurement of the Tear Film as a Diagnostic Tool for Meibomian Gland Dysfunction. Cornea 2013;32:1549–53. doi:10.1097/ICO.0b013e3182a7f3e1. [PubMed: 24097185]

[35]. Glasgow BJ, Marshall G, Gasymov OK, Abduragimov AR, Yusifov TN, Knobler CM. Tear lipocalins: potential lipid scavengers for the corneal surface. Invest Ophthalmol Vis Sci 1999;40:3100–7. [PubMed: 10586930]

[36]. Tragoulias ST, Anderton PJ, Dennis GR, Miano F, Millar TJ. Surface pressure measurements of human tears and individual tear film components indicate that proteins are major contributors to the surface pressure. Cornea 2005;24:189–200. [PubMed: 15725888]

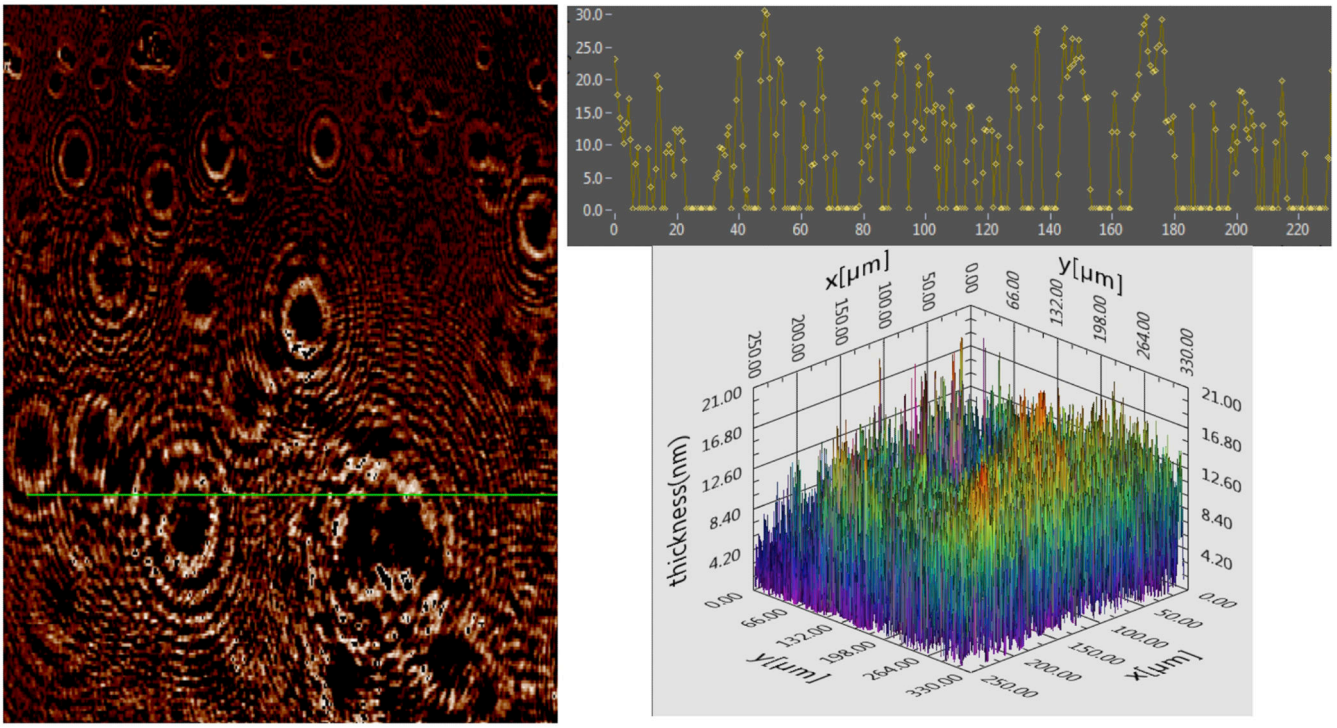

Figure 1.

Surface layer of pooled tears. Left: Two dimensional (2D) thickness map for pooled tears. The intensity (brightness) of the image pixel corresponds to the relative thickness. Top right, Histogram of thickness (z axis) derived from linear section at the x, y coordinates as depicted by the green line on the map. Bottom: 3D map of image thickness from another area, calculated from Ψ and Δ at various pixels in interpolation mode.

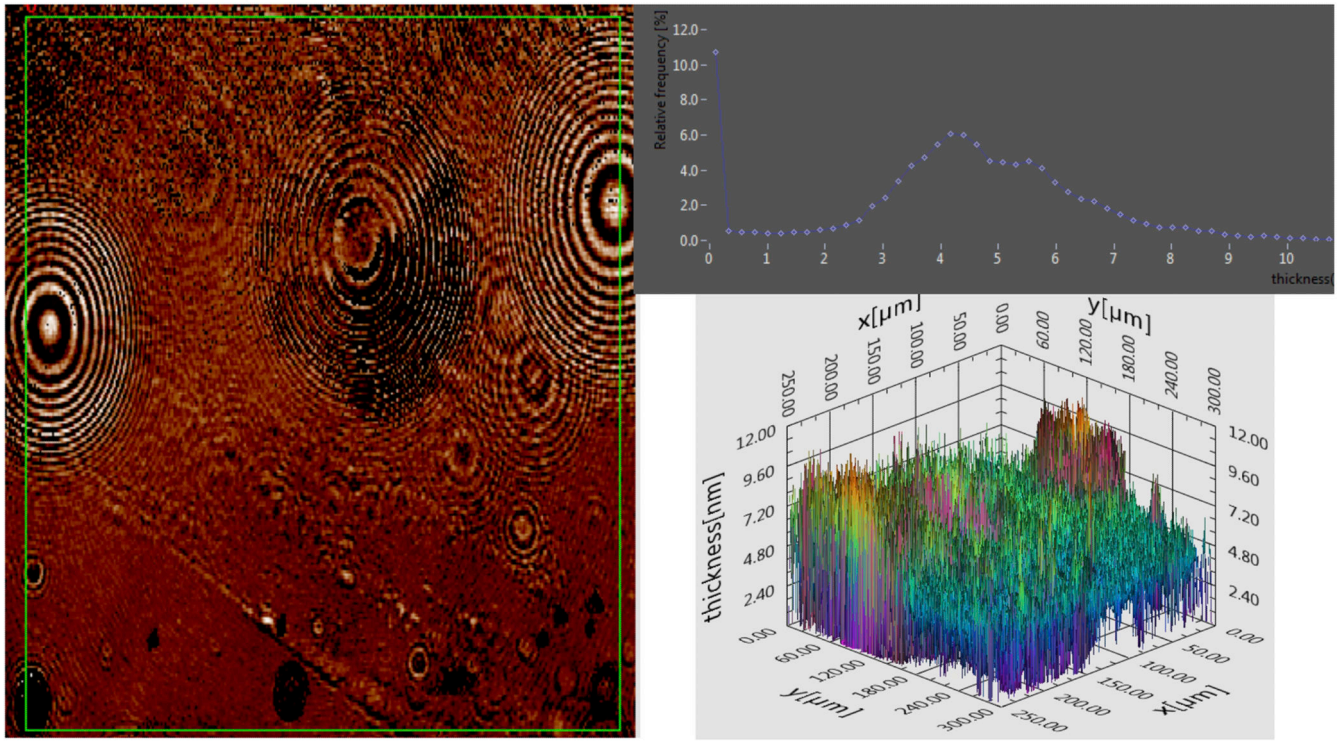

Figure 2.

Surface layer of one individual's tears analyzed immediately after collection. Left shows the 2 D map for thickness computed from the Ψ and Δ map. The intensity (brightness) reflects relative thickness. The green box represents the area from which data was extracted for the histogram (top right). The y axis represents the frequency of each thickness. Bottom right shows the 3 D map for thickness. Note in some cases the baseline is shifted upward due to an uneven aqueous subphase.

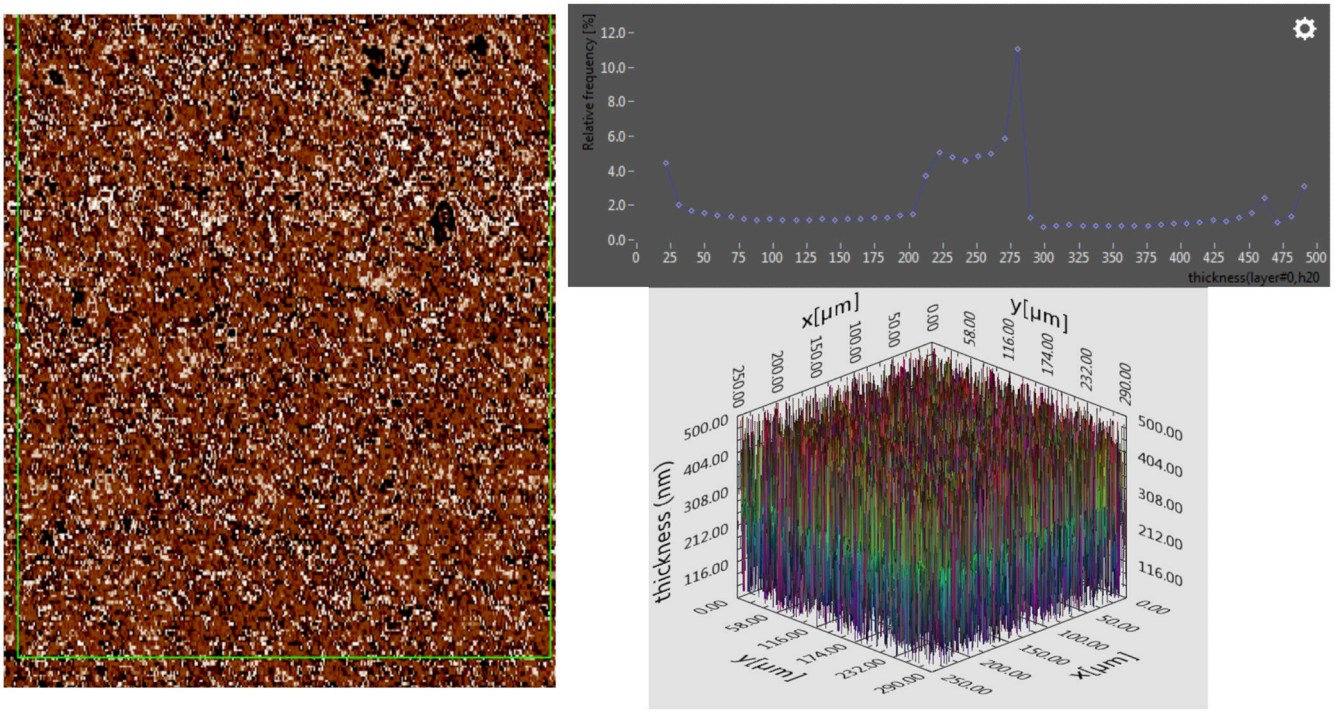

Figure 3.

Tears analysed immediately after collection from the same subject as shown in Figure 2, but collected one week later. Left, image map shows relative intensity from 21 nm (black) to 500 nm (white). Top right, histogram is taken from the area depicted in green. Bottom right, 3D map of thickness fit from Ψ and Δ at each pixel. Notice the baseline is slightly irregular.

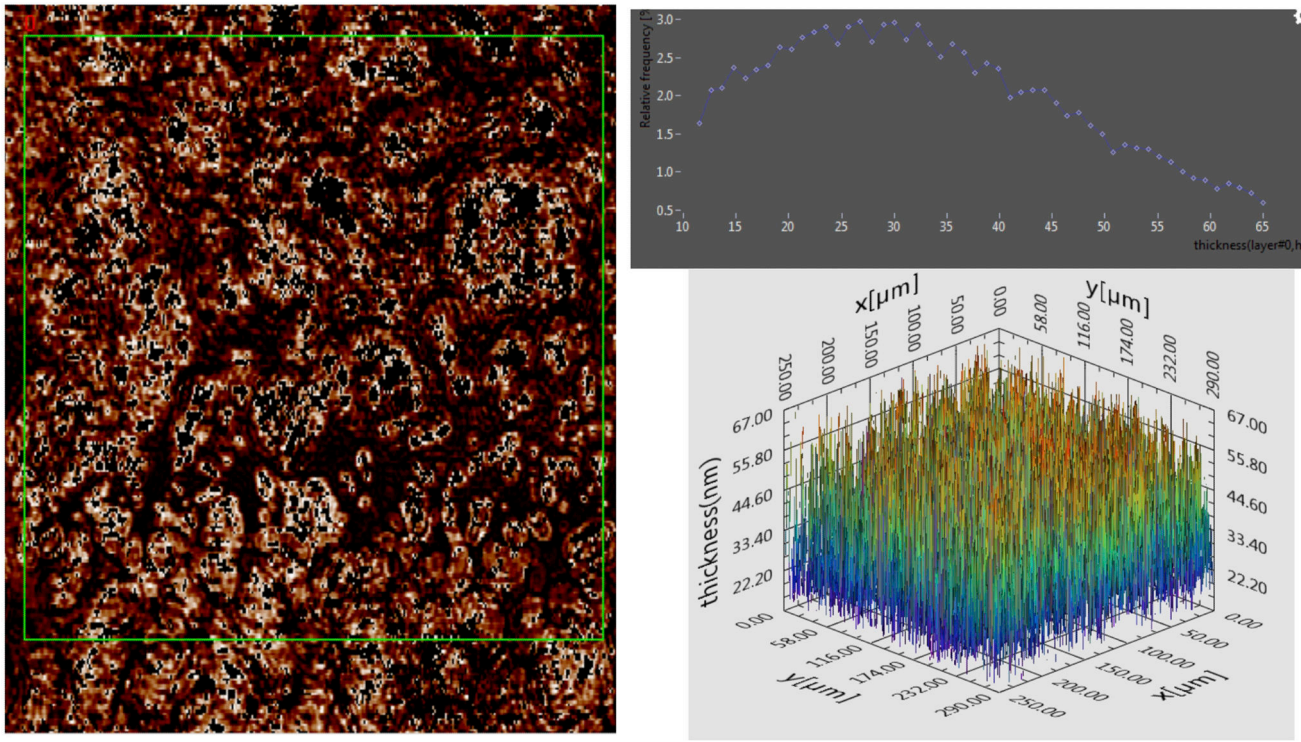

Figure 4.

Tears from an individual with dry eye disese. Left, 2D image of thickness map constructed from Ψ and Δ. The histogram from data bounded by the green box is shown in the histogram (top right). The 3D map of thickness is shown (bottom right).

Table 1.

Variation in Thickness Reported for the Surface Film on Tears

Reference	Method	Interpreted thickness (nm)
[1]■	Specular Reflection (color interference)	~100-370 (500)
[8]■	Specular Reflection (color interference)	102
[9]■ ■	Specular Reflection (color interference)	60-180
[10]■	Surface Potential vibrating glass plates	2-4
[11]■	Brewster Angle Microscopy	~2-10
[12]■	Specular Reflection (color interference	~100
[4]■	Specular Reflection (color interference)	75 (72% of normals)
[13]■	Microscopy and Reflectance	<20->120
[5]■	Ellipsometry (LED)	(150 +/− 7) theoretical
[6]■	OCT	20-60
[7]■	Interference (global fit from RGB values)	68

Table 2.

Thickness Ranges for Controls and Tear Sample in this Study

Sample	Thickness range (nm)
H20 with no surface layer (control)	0-.1
Monolayer of oleic acid on water (control)	1.1- 1.6
Monolayer of DPPC on water (control)	2.6- 2.8
Tears stored lots of 30 normal individuals	0-197
Tears (fresh, 4 normal individuals)	0-500
Tears (fresh 1 normal individual, 7 repeat measurements from same ROI)	0-110
Tears (fresh from individual with dry eye)	0-60